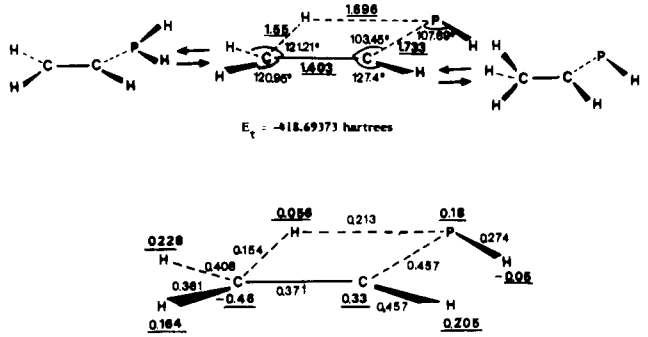


**Figure 9.** (Top) Transition-state geometry for the interconversion $HP{=}CHCH_3$–vinylphosphine. (Bottom) Mulliken populations: net total charges (underlined) and overlap populations.

between phosphirane and phosphaalkene. Although one of the P–C lengths is partially broken, the other presents a single-bond character 1.836 Å long and an overlap population of 0.19, very far from the value of 0.57 of the P=C double bond in $HP{=}C{-}HCH_3$. In addition, the 1,2-migration that occurs leads to hydrogen bridging between the two carbons in the transition state, since the two C–H bond lengths are 1.355 and 1.92 Å.

**Phosphirane–$CH_3P{=}CH_2$.** The phosphirane ↔ $CH_3P{=}CH_2$ interconversion mechanism corresponds to a scission of the C–C bond and a migration of the hydrogen bound to phosphorus.

The SCF calculations performed allow us to consider probably a two-step mechanism beginning with a scission of the C–C bond followed by formation of a ring-opened intermediate. Further insight into this mechanism may be obtained by examination of this structure, and we cannot account for this properly within an SCF approximation. No further attempt has been made because experimentally the opening of the phosphirane ring has been observed to occur with a cleavage of the P–C bond and not of the C–C bond.[24]

**$HP{=}CHCH_3$–$H_2PCH{=}CH_2$.** The barrier of the $HP{=}CHCH_3{-}H_2PCH{=}CH_2$ interconversion is higher than the above two, at 437.5 kJ·mol$^{-1}$, resulting from the occurrence of a 1,3-migration. As a result of this, the geometric characteristics of the transition state (Figure 9) correspond to a hydrogen in the process of migration, partially bound to both phosphorus (P–H = 1.696 Å) and the terminal carbon (C–H = 1.55 Å), the associated overlap populations being 0.213 and 0.154. It should also be noted that this migration occurs in the $\sigma$ plane with a practically flat transition state. The structure of the rest of the system is intermediate between the two isomers, i.e. a 1.403-Å C=C double bond and a P—C bond 1.733 Å long, at midway between those lengths of vinylphosphine of 1.83 Å and phosphaalkene of 1.647 Å (Figures 4 and 9).

## Conclusion

The data in this work have led to the definition of the essential characters of the mechanisms of addition and insertion of singlet phosphinidene on an olefin. The addition reaction occurs according to a highly symmetric least-motion path and with no activation energy. The insertion envisioned at the $\sigma$ level corresponds to a concerted mechanism with passage through a three-center transition state and an activation barrier of 25.1 kJ·mol$^{-1}$ after CI.

The energy values obtained for phosphirane, vinylphosphine, and phosphaalkenes monomethylated on carbon and methylated on phosphorus show that the last is the most stable isomer and that vinylphosphine is the least favored, even though the four values are similar. The analysis of the electronic and structural characteristics of the four systems and the determination of the transition states associated with the main interconversions have contributed data on the mechanisms that might occur during ring-opening 1,2- and 1,3-migration.

**Acknowledgment.** We thank the "Centre de Calcul Vectoriel pour la Recherche for generous allotments of computer time.

**Registry No.** PH, 13967-14-1; $C_2H_4$, 74-85-1; $H_2PCH{=}CH_2$, 58436-39-8; $HP{=}CHCH_3$, 107257-40-9; $CH_3P{=}CH_2$, 89149-01-9; phosphirane, 6569-82-0.

---

Contribution from the Institut für Anorganische und Analytische Chemie, Technische Universität Berlin, D-1000 Berlin 12, West Germany, and Institut für Physikalische Chemie der Universität Münster, D-4400 Münster, West Germany

# Molybdenum Cluster Chalcogenides $Mo_6X_8$: Intercalation of Lithium via Electron/Ion Transfer

E. Gocke,[†] R. Schöllhorn,*[†] G. Aselmann,[‡] and W. Müller-Warmuth[‡]

*Received October 2, 1986*

The electrochemical intercalation of lithium at 300 K into the rhombohedral molybdenum cluster chalcogenides $Mo_6X_8$ (X = S, Se) under formation of ternary phases $Li_xMo_6X_8$ has been investigated with respect to the changes of composition, structure, and bonding. Complete $^7$Li NMR phase diagrams have been established, and thermodynamic data are given. Diffusion coefficients and NMR dipolar line width demonstrate a rather high lithium ionic mobility; the reactions are fully reversible. Results are closely similar for the sulfide and selenide system. Four distinct rhombohedral phases with $x$ = 1, 3, 3.8, and 4 could be identified. The transition from $x$ = 1 to $x$ = 3 is correlated with a significant increase in unit cell volume and an unusually strong decrease in NMR line shift. The latter has been interpreted in terms of a partial charge transfer with formation of triangular $(Li_3)^{2+}$ clusters, i.e. $(Li_3)^{2+}[Mo_6S_8]^{2-}$. For $Li_4Mo_6S_8$ the NMR shift changes again abruptly in the inverse sense to values indicating "normal" $Li^+$ ions. This is attributed to the loss in symmetry of the lithium clusters as well as the tendency for quantitative saturation of the $Mo_6$ clusters with 24 electrons (metal/semiconductor transition).

## Introduction

Binary and ternary molybdenum cluster chalcogenides (Chevrel phases) with the composition $Mo_6X_8$ and $A_xMo_6X_8$ (X = S, Se, Te; A = main-group or transition metal) exhibit unusual structural and physical properties and have been investigated intensively after it became apparent that many of these phases are superconducting materials with high critical temperatures and high critical magnetic fields.[1,2] The structure of the binary phases can be described by a three-dimensional arrangement of $Mo_6X_8$ units, which them-

* To whom correspondence should be addressed.
[†] Technische Universität Berlin.
[‡] Universität Münster.

(1) Yvon, K. In *Current Topics in Materials Science*; Kaldis, E., Ed.; North Holland: Amsterdam, 1979, Vol. II, p 53.
(2) Fischer, Ø, Maple, M. B., Eds.; *Superconductivity in Ternary Compounds*; Springer Verlag: Berlin, West Germany, and Boston, MA, 1982, Vols. I and II.

0020-1669/87/1326-1805$01.50/0 

**Table I.** Rhombohedral and Hexagonal Lattice Parameters of Ternary Lithium Phases $Li_xMo_6X_8$

| $x$ | X | $a_R$, pm | $\alpha_R$, deg | $10^{-6}V_R$, pm$^3$ | $a_H$, pm | $c_H$, pm | $c/a$ | $10^{-6}V_H$, pm$^3$ |
|---|---|---|---|---|---|---|---|---|
| 0 | S | 643.0 | 91.27 | 266.0 | 919.2 | 1088.9 | 1.1846 | 796.7 |
| 1 | S | 646.7 | 92.25 | 269.8 | 931.6 | 1076.4 | 1.1554 | 809.0 |
| 3 | S | 663.8 | 94.29 | 289.9 | 972.5 | 1060.3 | 1.0903 | 868.5 |
| 3.8 | S | 659.6 | 94.23 | 284.6 | 970.7 | 1053.9 | 1.0857 | 860.0 |
| 4 | S | 664.7 | 94.52 | 290.7 | 976.6 | 1056.2 | 1.0815 | 872.5 |
| 0 | Se | 666.0 | 91.70 | 294.9 | 955.5 | 1119.6 | 1.1717 | 885.2 |
| 1 | Se | 672.4 | 92.23 | 303.3 | 969.3 | 1118.5 | 1.1539 | 910.2 |
| 3 | Se | 691.5 | 94.42 | 327.5 | 1015.8 | 1100.0 | 1.0829 | 983.1 |
| 4 | Se | 692.3 | 94.40 | 328.7 | 1015.2 | 1103.5 | 1.0870 | 985.0 |

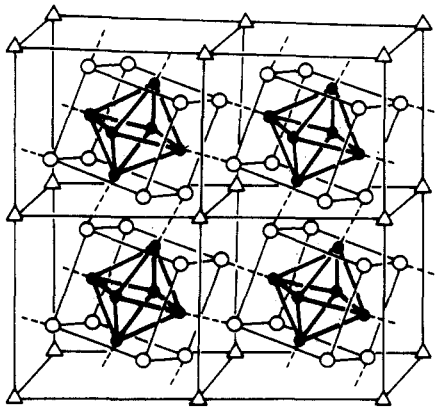

**Figure 1.** Structure scheme of binary molybdenum cluster chalcogenides $Mo_6X_8$ (X = S, Se, Te): ● = Mo; ○ = X; triangles represent vacant "channel" positions at the unit cell origin.

selves consist of $X_8$ cubes surrounding the distorted $Mo_6$ octahedra. This framework system leads to intersecting "channels" of vacant lattice sites along the three rhombohedral axes, which are (partially) occupied in the case of ternary phases by the metal atoms A (Figure 1). It has been shown recently that the $Mo_6X_8$ cluster phases moreover exhibit remarkable properties in terms of *chemical reactivity*. They are able to undergo reversible topotactic redox reactions at ambient temperature via electron/ion transfer according to eq 1.[3,4] The electrons are accepted by empty levels

$$xA^+ + xe^- + \square_n[Mo_6X_8] \rightleftarrows (A^+)_x\square_{n-x}[Mo_6X_8]^{x-} \quad (1)$$

of appropriate energy of the host band, which acts as an electron sink, and the matrix becomes a macroanion $[Mo_6X_8]^{x-}$. The negative excess charge is compensated by the simultaneous uptake of mobile cations $A^+$, which occupy empty sites □ in the lattice channels. In the intercalated state the system represents thus an electronic/ionic conductor system. The intercalation can be performed either by chemical reaction or by electrochemical action in appropriate electrolytes. The uptake of guest cations is limited by the effective diameter of the lattice channels; the critical radius increases from X = S to X = Te. The process described allows the reversible modification of the physical properties of the $Mo_6X_8$ matrix by chemical reactions at ambient temperature.

One aspect of particular interest with respect to the chemical reactivity of these systems is the upper stoichiometry limit $x_{max}$ of the guest cations. The latter can be treated in a simple model in terms of a competition between geometrical and electronic restraints.[4,5] For small ions the structure provides formally 12 potential lattice sites around the unit cell origin with distorted tetrahedral symmetry.[1,2] If repulsive electrostatic interaction between the cations is taken into account, a maximum number of six cations per $Mo_6X_8$ unit can be expected for monovalent species. In electronic terms, however, the maximum charge transfer predicted is equivalent to $4e/Mo_6X_8$, resulting in the maximal insertion of, e.g., four monovalent cations $A^+$ or two bivalent cations $A^{2+}$. This is a consequence of the ionic model discussed by Yvon,[1] which considers the electron-deficient $Mo_6$ cluster in $Mo_6X_8$ that can take up formally four additional electrons in order to establish 12 two-electron Mo–Mo bonds. Band structure calculations are in agreement with this model.[6]

The smallest monovalent metal ion that can be intercalated into the $Mo_6X_8$ host lattice is $Li^+$ with an ionic radius of 62 pm. Since it can be expected that for $Li^+$ steric constraints will be of minor influence, the system $Li/Mo_6X_8$ represents a crucial test case for an investigation of the charge-transfer model mentioned. The first investigations on the intercalation of Li into $Mo_6S_8$ were performed by electrochemical techniques.[7] Cyclic voltammetric studies revealed the presence of two Li phases and a high mobility of Li at 300 K; galvanostatic titration led to the identification of rhombohedral $Li_{0.8}Mo_6S_8$ and $Li_xMo_6S_8$ with $2.4 < x < 3.6$. Intercalation via solutions of lithium metal in liquid $NH_3$ yielded similar lattice parameters of the products, but an upper limit of $x = 6$.[8] In subsequent electrochemical studies and intercalation of Li via butyllithium[9,10] the existence of two Li phases was confirmed, but varying phase ranges had been observed and a triclinic terminal phase was reported.[11] Since the Li system is of particular importance for the charge-transfer problem, we have undertaken a thorough study, concerning structural and compositional changes, with $Mo_6S_8$ and $Mo_6Se_8$ as the host lattice. These investigations have been supplemented by extensive $^7$Li NMR studies, which have turned out to be a highly useful analytical tool for establishing the phase diagrams and the temperature-dependent dynamics of the guest species. They also led us to the observation of a series of unusual features with respect to chemical shift, line width, relaxation data, and their temperature dependence. The results present evidence for an unexpected and rather complex electronic behavior of the system under investigation.

## Experimental Section

The starting materials $Mo_6S_8$ and $Mo_6Se_8$ were prepared from the ternary phases $Cu_2Mo_6S_8$ and $Cu_2Mo_6Se_8$. The latter were obtained by heating the elements (stoichiometric ratio) in sealed quartz ampules for 24 h to 450 °C and thereafter for 24 h to 700 °C. After each heating period, the loose powder in the ampules was agitated in order to achieve homogeneous products. Opening of the ampules and treatment of the prereacted material in a ball mill was observed to introduce small

(3) Schöllhorn, R. *Angew. Chem.* **1980**, *92*, 1015; *Angew. Chem., Int. Ed. Engl.* **1980**, *19*, 983.
(4) Schöllhorn, R. In *Inclusion Compounds*; Atwood, J. L.; Davis, J. E. D., MacNicol, D. D., Eds.; Academic: London, New York, 1984; Vol. I, p 249.
(5) Schöllhorn, R. In *Chemical Reactions in Organic and Inorganic Constrained Systems*; Setton, R., Ed.; D. Reidel: Dordrecht, The Netherlands, 1986; p 323.
(6) Hughbanks, T.; Hoffmann, R. *J. Am. Chem. Soc.* **1983**, *105*, 1150. Andersen, O. K.; Klose, W.; Nohl, H. *Phys. Rev. B: Solid State* **1978**, *17*, 1209.
(7) Schöllhorn, R.; Kümpers, M.; Besenhard, J. O. *Mater. Res. Bull.* **1977**, *12*, 781.
(8) Schöllhorn, R.; Kümpers, M.; Lerf, A.; Umlauf, E.; Schmidt, W. *Mater. Res. Bull.* **1979**, *14*, 1039.
(9) Tarascon, J. M.; Di Salvo, F. J.; Murphy, D. W.; Hull, G. W.; Rietman, E. A. Waszczak, J. V. *J. Solid State. Chem.* **1984**, *54*, 204.
(10) Behlok, R. J.; Robinson, W. R. *Mater. Res. Bull.* **1983**, *18*, 1069. Behlok, R. J.; Kullberg, M. L.; Robinson, W. R. *Chemistry and Uses of Molybdenum, Proceedings of the 4th International Conference*; Barry, H. F., Mitchell, P. C. H., Eds.; Climax Molybdenum Co.: Ann Arbor, MI, 1982.
(11) McKinnon, W. R.; Dahn, J. R. *Phys. Rev. B: Condens. Matter.* **1985**, *31*, 3084.
(12) Coleman, S. T.; McKinnon, W. R.; Dahn, J. R. *Phys. Rev. B: Condens. Matter.* **1984**, *29*, 4147.
(13) Riekel, C.; Reznik, H. G.; Schöllhorn, R. *J. Solid State Chem.* **1980**, *34*, 253.
(14) Riekel, C.; Schramm, W.; Schöllhorn, R., submitted for publication. Schramm, W. Dissertation Universität Münster 1981.

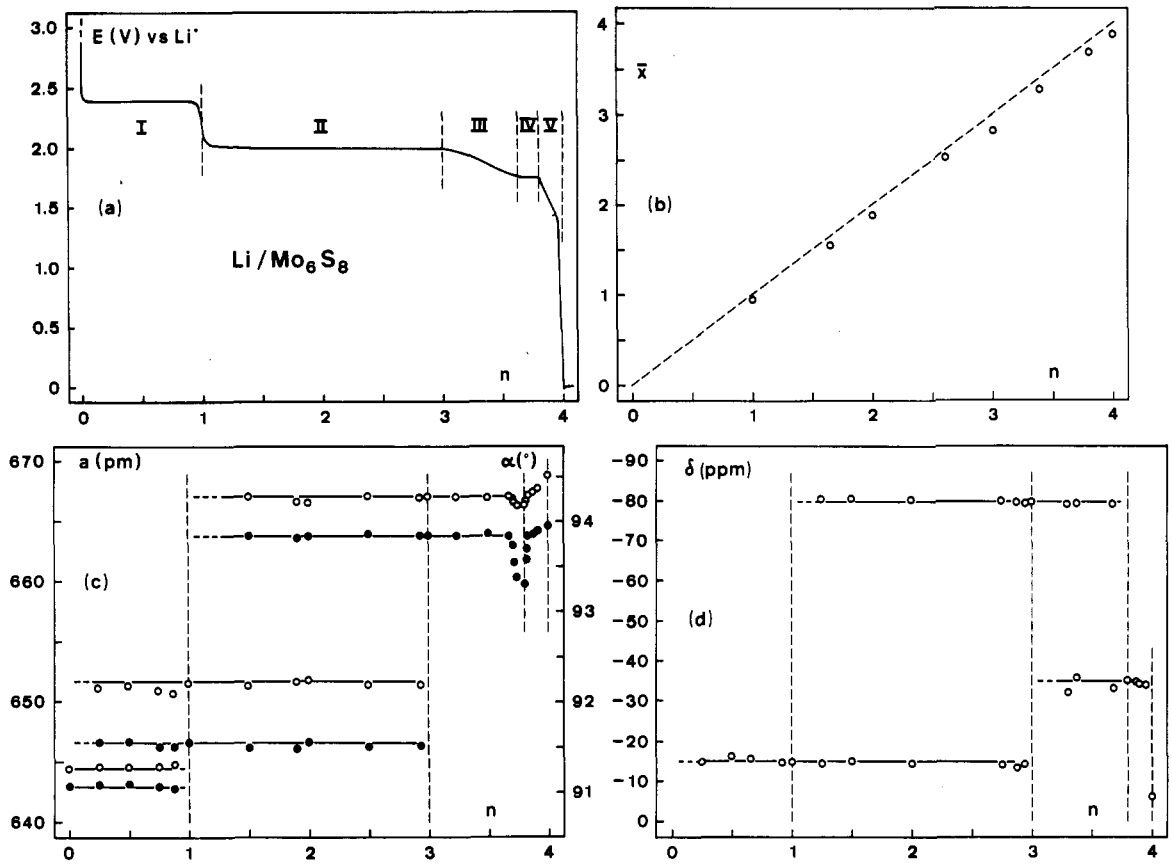


**Figure 2.** Formation of $Li_xMo_6S_8$ by galvanostatic cathodic reduction of $Mo_6S_8$ electrodes in aprotic $Li^+$ electrolyte at 300 K (nominal current density 100 $\mu A\ cm^{-2}$): (a) change of potential $E$ (vs. $Li^0$) of the working electrode with the charge transfer $n$ ($e/Mo_6S_8$); (b) correlation between the integral Li content $\bar{x}$ of the reaction products with the charge transfer $n$; (c) change of rhombohedral lattice parameters with $n$ ($a_R$ = ●, $\alpha_R$ = ○); (d) $^7Li$ NMR phase diagram (300 K), change of the chemical shift $\delta$ with $n$ (reference: saturated aqueous LiCl solution).

amounts of oxygen. The final heating mode was 1100 °C (sulfide) and 1200 °C (selenide) for 24 h with subsequent slow cooling over the course of 10 days. The purity of the elements used was better than 99.9%. Rhombohedral lattice parameters of the ternary copper phases ($Cu_2Mo_6S_8$: $a_R$ = 651.8 pm, $\alpha_R$ = 95.19°. $Cu_2Mo_6Se_8$: $a_R$ = 678.1 pm, $\alpha_R$ = 94.73°) agreed with literature data.[2] Treatment of the copper compounds with aqueous $FeCl_3$/0.1 N HCl solution led to the quantitative removal of Cu with formation of $Mo_6S_8$ and $Mo_6Se_8$ (lattice parameters given in Table I). Attempts were also made to perform the deintercalation of Cu by treatment of the Cu phases with $I_2/CH_3CN$. The X-ray pattern indicated, however, a few weak lines of $MoS_2$ and $MoSe_2$, respectively, which were absent in the case of $FeCl_3$/HCl as the oxidant. EDAX studies confirmed the absence of copper in both cases. Analytical data were obtained by wet analysis, spectrophotometry, atomic absorption spectrometry, and microanalysis. The values found for the binary phases were as follows. Anal. Found (calcd) for $Mo_6S_8$: Mo, 68.94 (69.18); S, 30.90 (30.82). Found (calcd) for $Mo_6Se_8$: Mo, 47.69 (47.68); Se, 52.55 (52.32). Direct preparation of the thermodynamically stable binary phase $Mo_6Se_8$ from the elements led to products with low reactivity; we assume that this is a consequence of defects blocking the empty lattice channels.

For control purposes the lithium content was routinely checked also by acid/base titration after the decomposition of the Li phases in distilled water according to

$$Li_xMo_6X_8 + xH_2O \rightarrow Mo_6X_8 + xLiOH + (x/2)H_2 \qquad (2)$$

X-ray powder measurements were made by the Simon–Guinier technique from samples sealed in lithium borate glass capillaries. Because of the extreme sensitivity of the intercalated phases to oxygen and water, all operations had to be carried out in closed systems under argon atmosphere. The binary phases $Mo_6X_8$ were similarly stored under inert-gas atmosphere, since we found that on exposure of these compounds to air slow oxidation (catalyzed by Mo) proceeds with formation of $H_2SO_4$ and $H_2SeO_4$, respectively.

Electrochemical reactions were performed at 300 K in three electrode galvanic cells with commercial and homemade equipment to monitor current and potential. Galvanostatic titration, potentiostatic reaction with integration of the charge consumed, slow voltammetry and cyclic voltammetry, short circuit runs, and EMF measurements (equilibrium potentials) were used for the electrochemical study of the reactions. The working electrodes consisted of pressed polycrystalline samples with 1% wt Teflon (blank tests showed Teflon to be inert under the conditions applied) as binder. Above a critical stoichiometry the reactions are correlated with a strong volume increase; in the absence of Teflon the resulting mechanical stress leads to regions of the electrode that lose electronic contact, thus leading to a significant error in yield. Dried $LiClO_4$ in high-purity propylene carbonate (residual water content 26.9 ppm as determined by Karl Fischer titration) served as the electrolyte. For comparison purposes with respect to composition and structure several samples of defined stoichiometry were also prepared by reaction of $Mo_6X_8$ with butyl lithium (1.5 M solution in hexane) and with lithium dissolved in liquid $NH_3$ at −30 °C. The products obtained were identical with those prepared electrochemically, except for slight line broadening, which is reduced on annealing at 150 °C. For small samples intercalated electrochemically at low current densities, the potentials measured are very close to the equilibrium values in the range $0<\bar{x}<3$.

The $^7Li$ NMR measurements were performed at 116.59 MHz on a Bruker CXP 300 FT spectrometer. As an external reference for the chemical shift determination we utilized aqueous solutions of LiCl. The NMR lines appear so narrow at room temperature that only the isotropic part of the shift is observed. The chemical shift in these compounds is always negative ("downfield" shift or "paramagnetic" shielding), but it varies between −6 and −86 ppm at 300 K. Further details and results of the NMR studies will be published elsewhere.[15]

## Results and Discussion

**I. The Sulfide System $Li/Mo_6S_8$: Formation, Structural Changes, and Phase Diagrams.** The potential/charge-transfer diagram for the electrochemical intercalation of $Li^+$ into the $Mo_6S_8$ host lattice by cathodic reduction in a galvanic cell

$$Li^0|LiClO_4, \text{ propylene carbonate}|Mo_6S_8$$

is given in Figure 2a. Parts b–d of Figure 2 illustrate the cor-

(15) Aselmann, G.; Müller-Warmuth, W.; Gocke, E.; Schöllhorn, R. *Z. Phys. Chem. (Munich)*, in press.

responding compositional and structural changes and the $^7$Li NMR chemical shift data observed in the course of the reaction by taking samples at given values of the specific electrochemical charge transfer $n$ ($e/Mo_6S_8$). The end point of the reaction is attained after a transfer of $4e/Mo_6S_8$, where the electrode potential (under the conditions of galvanostatic titration at low current density) becomes identical with the potential of the lithium metal reference electrode and metal deposition is observed. Former electrochemical studies by us[7] and by other authors[9] yielded significantly lower values; this discrepancy has to be attributed to the fact that the overall reaction is correlated with a strong change in unit cell volume (Table I), resulting in a partial mechanical disintegration of the polycrystalline electrode material and thus in regions that lose electrical contact with the cathode lead. This obstacle can be avoided by appropriate techniques (cf. Experimental Section). Figure 2b demonstrates that no side reactions occur: the charge transfer agrees well according to $n = \bar{x}$ with the integral lithium content $\bar{x}$ of the reaction products as determined analytically. Short circuit cell runs and reactions in potentiostatic mode (integration of current) confirmed as well maximum transfer of $4e/Mo_6S_8$ and a chemical composition of the terminal phase corresponding to $Li_4Mo_6S_8$. The maximum charge transfer observed is thus in formal agreement with the predictions from the ionic structure model[1] and the band structure calculations[6] for $Mo_6X_8$ type systems.

The potential/charge-transfer curve of Figure 2a represents an isothermal cross section of the phase diagram at 300 K and can be divided formally into sections I–V according to changes of slope in potential that indicate a rather complex system. In terms of thermodynamics the potential plateaus appearing in sections I, II, and IV should represent two-phase systems with $\Delta G$ = constant. The corresponding structural data over the entire phase range are given in Figure 2c. Table I presents lattice parameters and unit cell volumes of the starting phase and of ternary Li compounds. It is seen that region I is clearly characterized by the coexistence of two phases: $Mo_6S_8$ and a line phase $Li_1Mo_6S_8$ (eq 3) with no detectable phase width. The change in

$$Li^+ + e^- + Mo_6S_8 \rightleftarrows Li_1^+[Mo_6S_8]^- \quad (3)$$

unit cell volume and the distortion of the original lattice is relatively small as compared to the subsequent phases; the formation of a $Li_1$ phase may thus be understood in terms of the competition between loss in lattice energy by distortion and gain in Coulomb energy by the simultaneous insertion of more than one lithium ion. The observation of a two-phase system in region I is at variance with the report of the existence of a solid solution of $Li_xMo_6S_8$ ($0 \leq x \leq 1$) by Mc Kinnon that has been discussed in terms of a lattice gas model.[12] The latter results have been obtained by in situ electrochemical studies on an X-ray diffractometer. A problem with this technique is, however, that X-ray radiation has a low penetration depth and yields only structural information on regions close to the electrode surface, which may lead to erroneous conclusions, e.g. in two-phase regions. Since the lattice parameter change is rather small, an overlap of closely neighboring Bragg peaks varying in intensity with $n$ may simulate a continuous change in structure at lower instrument resolution. Previous experiments by us on "in situ" studies of electrochemical cells by neutron diffraction demonstrated that reliable bulk structural information can be obtained by an appropriate arrangement of the galvanic cell.[13] We have therefore performed a supplementary study of the $Li/Mo_6S_8$ system by neutron powder diffraction (high-flux reactor at the ILL, Grenoble, France), whose results are in agreement with the existence of a two-phase system in region I.[14]

Region II represents similarly a two-phase region with the coexistence of the phases $Li_1Mo_6S_8$ and $Li_3Mo_6S_8$ leading to a further uptake of 2e and two $Li^+$ ions (eq 4). This transition

$$2Li^+ + 2e^- + Li_1Mo_6S_8 \rightleftarrows Li_3Mo_6S_8 \quad (4)$$

is accompanied by a significant change in lattice parameters and an increase in unit cell volume of 9.5% (Table I). The width of the plateau regions I and II and thus the stoichiometry of the corresponding Li phases were confirmed independently by potentiostatic measurements and integration of the charge consumed at the plateau potential. The observation of two two-phase regions is in qualitative agreement with our former studies by electrochemical methods and by reaction of $Mo_6S_8$ with Li° in liquid $NH_3$; the phase limits reported in this work are lower, however.[7,8]

The interpretation of the phase diagram in regions III–V (eq 5) is less straightforward, and to some extent contradictory evi-

$$Li^+ + e^- + Li_3Mo_6S_8 \rightleftarrows Li_4Mo_6S_8 \quad (5)$$

dence has been obtained. The data from Figure 2a suggest a one-phase system $Li_xMo_6S_8$ with $3 \leq x \leq 3.6$, a two-phase system $3.6 \leq x \leq 3.8$, and a second one-phase system $3.8 \leq x \leq 4.0$. The changes in lattice parameters (Figure 2c, Table I) are very small, however, so that a reliable distinction for region IV between a two-phase or one-phase system is not possible. The general trends in structural changes are, however, clear and are supported by a large number of measurements (Guinier technique) at given $n$ values. In section III (Figure 2a) up to a charge transfer of $3.6e/Mo_6S_8$ the rhombohedral lattice parameters $a_R$ and $\alpha_R$ and the unit cell volume are identical with those of the $Li_3$ phase within the limits of accuracy. In section IV a minimum of $a_R$ and $\alpha_R$ is observed close to $n = 3.8$, while a slight increase in the lattice parameters (relative to those of $Li_3$) is found in the terminal region V. The hexagonal $c/a$ ratio decreases, however, continuously from $Li_3$ to $Li_4$ as expected. The final lattice parameters for $Li_4Mo_6S_8$ correspond well with those given by Robinson et al. for the same phase prepared from $Mo_6S_8$ and butyllithium.[10] We cannot confirm the results of Mc Kinnon et al., who report a triclinic phase.[11]

The reactions just discussed and described by eq 3–5 are completely reversible without hysteresis. On anodic oxidation the same sequence of reactions is found in the inverse direction; the final product after a charge transfer of $4e/Li_4Mo_6S_8$ is the binary phase $Mo_6S_8$ with lattice parameters identical with those given in Table I.

**II. NMR Studies on the Sulfide System.** In the course of our attempts to apply additional methods to the systems under discussion for further characterization (in particular with respect to regions III–V) solid-state $^7$Li NMR turned out to be a highly valuable tool not only for the investigation of the location and temperature-dependent dynamics of $Li^+$ in the host lattice but also for the analysis of the phase diagram and the control of purity of the samples obtained. Due to the relatively high mobility of Li in $Li_xMo_6S_8$ at 300 K and the excellent resolution of the instrument used, even minor amounts of phases present in mixtures could be detected readily. Figure 2d represents a complete $^7$Li NMR phase diagram of the intercalation process. For region I (Figure 2a) $Li_1Mo_6S_8$ is observed with a signal exhibiting a narrow central line with quadrupole satellites and a chemical shift of $\delta = -15$ (Figure 2d, 3). In region II the NMR data show clearly the coexistence of two signals related to $Li_1Mo_6S_8$ and $Li_3Mo_6S_8$ varying in relative intensity, the latter showing only one central line with $\delta = -80$. For $n = 3$ only the signal of $Li_3Mo_6S_8$ is observed. In the following section $3 \leq n \leq 3.8$ (i.e. regions III and IV) two signals are detected, varying in relative intensity with increasing $n$: one is the line with $\delta = -80$ identified before as $Li_3Mo_6S_8$, while the second line exhibits a shift of $\delta = -35$. For $n = 3.8$ only one signal ($\delta = -35$) is measured. Reoxidation of $Li_{3.8}Mo_6S_8$ to $Li_3Mo_6S_8$ yields again a single signal characteristic of the latter phase. This observation is rather surprising, since the electrochemical data (Figure 2a) suggest a one-phase range for $3 \leq x \leq 3.6$.

In the following section, region V, only the signal with $\delta = -35$ is observed up to $n \sim 3.95$, while a sudden shift drop down to a value of $\delta = -6$ is found for the fully intercalated phase $Li_4Mo_6S_8$. The reactions are completely reversible in terms of the NMR data. On extended discharge of the working electrode at potentials <1 V some irreversible side reactions occur, however, as indicated by the appearance of additional $^7$Li NMR signals at lower shift values (−25 to −55 ppm). These are assumed to originate from catalytic solvent decomposition and formation of organic lithium

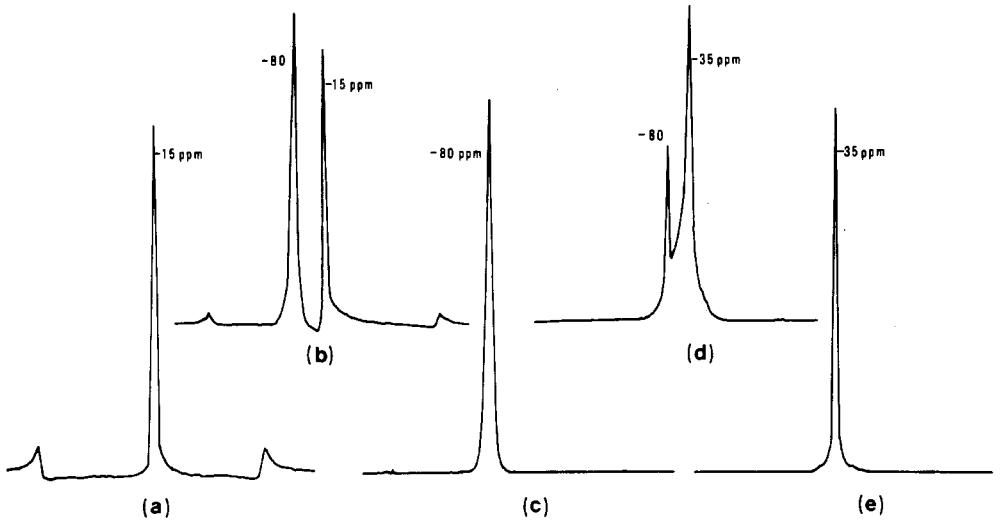


**Figure 3.** $^7$Li NMR spectra of the $Li/Mo_6S_8$ system for selected charge transfer values: (a) $n = 1$, $Li_1Mo_6S_8$; (b) $n = 2$, $Li_1Mo_6S_8 + Li_3Mo_6S_8$; (c) $n = 3$, $Li_3Mo_6S_8$; (d) $n = 3.5$, $Li_3Mo_6S_8 + Li_{3.8}Mo_6S_8$; (e) $n = 3.8$, $Li_{3.8}Mo_6S_8$.

compounds. In the absence of electrolyte no further change in the NMR signal is observed even after extended storage time (2 years).

**III. The Phase $Li_3Mo_6S_8$.** $Li_1Mo_6S_8$ appears to be quite "normal" with respect to structural and NMR results. There is only a relatively small change in unit cell volume from $Mo_6S_8$ to $Li_1Mo_6S_8$; the chemical shift of $\delta = -15$ is close to that of LiCl. The compound can thus be described by an ionic formula as $Li^+[Mo_6S_8]^-$, i.e. quantitative transfer of one electron to the host matrix band. $Li_3Mo_6S_8$ exhibits, however, some unusual features that require a separate discussion: (i) the strong change in unit cell volume of 9.5% relative to $Mo_6S_8$; (ii) the observation that in the NMR phase diagram $Li_3Mo_6S_8$ is clearly a line phase, while the electrochemical data suggest a nonstoichiometric phase with a lower limit of $x = 3$; (iii) an extreme shift of the $^7$Li NMR line of $\delta = -80$ at 300 K; (iv) a strong temperature dependence of the line shift; (v) nonclassical behavior of the spin–lattice relaxation data, i.e. a lower slope for the temperature dependence of the relaxation rates on the high-temperature branch as compared to the low-temperature branch. Moreover, the maxima of the relaxation rates are found at temperatures unusually low for lithium ionic conductors.[15]

We shall discuss here first the basic structural change and the related thermodynamics, thereafter examine the NMR data and the Li lattice sites, and finally try to develop a model to interpret the extreme shift value.

The fact that an isometric framework structure is able to undergo a volume change of 9.5% in a reversible topotactic reaction is quite remarkable. The magnitude of this change is larger than that observed for all other $A_xMo_6S_8$ compounds with monovalent ions reported so far as can be seen from Figure 4a. Among the ternary phases (prepared by *thermal* reaction) with large di- and trivalent cations only $Ba_1Mo_6S_8$ exhibits a slightly larger unit cell volume change of 10.2%.[16] The transition $Li_1 \rightarrow Li_3$ is also correlated with significant changes of the rhombohedral angle and the $c/a$ ratio of the hexagonal cell (Table I).

The thermodynamics of the phase changes are given in Table II. Although the existence of a large region with flat potential and a relatively high cell voltage (Figure 2a) are of interest for the application of these phases as reversible electrodes in secondary batteries, the Gibbs free energy of reaction, $\Delta G$, is relatively low. If we compare $\Delta G$ for the formation of $Li_1Mo_6S_8$ and $Li_1TiS_2$ (−206 kJ mol$^{-1}$)[17] and normalize to the same sulfur content, the energy gain ratio is ca. 1:4. The free energy released per intercalated Li is lower on going from $Li_1$ to $Li_3$. The existence of an intermediate $Li_1$ phase can be rationalized by the following arguments: at low Li concentration only a small distortion of the lattice is necessary in order to intercalate one $Li_+$ ion per unit cell with an asymmetric coordination as indicated the quadrupole splitting of the NMR signal. Further insertion of $Li^+$ is possible only at a threshold value of $x = 3$ with a strong distortion of the lattice but a simultaneous gain in the Coulomb interaction.

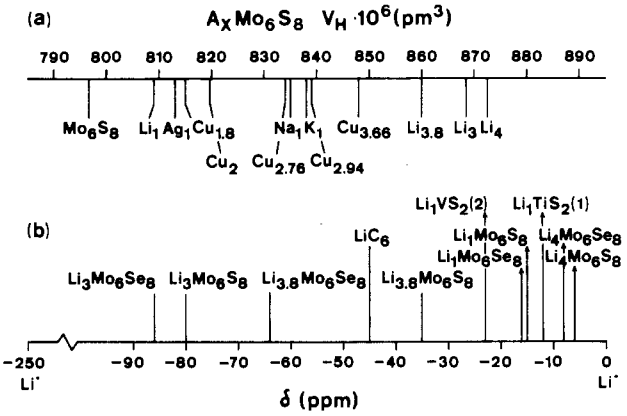


**Figure 4.** (a) Hexagonal unit cell volumes $V_H$ of $Mo_6S_8$ and of ternary phases $A_xMo_6S_8$ with monovalent guest ions A = Li, Na, K, Ag, Cu. (b) $^7$Li NMR chemical shift values of ternary lithium phases $A_xMo_6X_8$ (X = S, Se), $Li_1TiS_2$, $Li_1VS_2$, and $LiC_6$: (1) = ref 20, (2) = ref 21.

**Table II.** Free Energies of Formation ($\Delta G$) of Ternary Phases $Li_xMo_6X_8$ and Corresponding EMF Values ($T$ = 300 K)

| reaction | $\Delta G$, kJ mol$^{-1}$ | EMF, V |
|---|---|---|
| $Li + Mo_6S_8 \rightleftarrows Li_1Mo_6S_8$ | −230 | 2.38 (8) |
| $2Li + Li_1Mo_6S_8 \rightleftarrows Li_3Mo_6S_8$ | −386 | 2.00 (2) |
| $3Li + Mo_6S_8 \rightleftarrows Li_3Mo_6S_8$ | −616 | |
| $Li + Mo_6Se_8 \rightleftarrows Li_1Mo_6Se_8$ | −207 | 2.15 (0) |
| $2Li + Li_1Mo_6Se_8 \rightleftarrows Li_3Mo_6Se_8$ | −367 | 1.90 (1) |
| $3Li + Mo_6Se_8 \rightleftarrows Li_3Mo_6Se_8$ | −574 | |

It is known that the presence of small cations in $Mo_6S_8$ leads via deformation of the $Mo_6S_8$ matrix to the generation of 12 distorted tetrahedral sites around the unit cell origin.[1,2] These positions can be divided into two concentric sets of six sites (pleated hexagonal rings with their planes perpendicular to the threefold lattice axis). For $Cu_xMo_6S_8$ a tendency for depopulation of the inner rings with increasing copper concentration has been found.[1] For $Li_1Mo_6S_8$ it can be assumed that the Li atom is in an asymmetric position on the inner ring close to the sulfur atoms on the threefold symmetry axis, which explains the difference of the NMR quadrupole coupling constants for the compounds with S and Se. Recently a neutron powder diffraction study has been

(16) Chevrel, R.; Sergent, M.; Prigent, J. *J. Solid State Chem.* **1971**, *3*, 515.
(17) Whittingham, M. S. *Prog. Solid State Chem.* **1978**, *12*, 41.

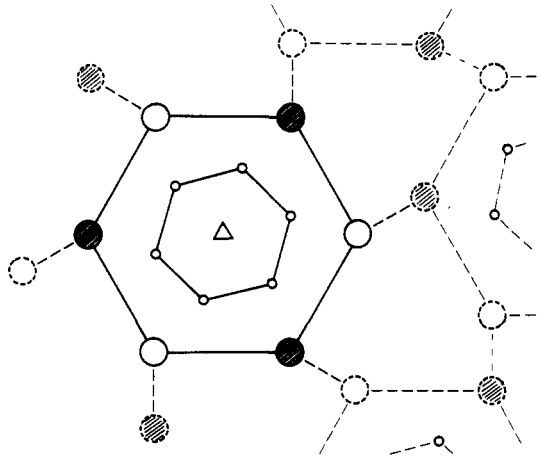

**Figure 5.** Scheme of lattice sites around the unit cell origin in $Li_3Mo_6S_8$: △, trigonal axis; inner positions, small circles; outer positions, large circles, filled positions, proposed Li sites; hatched circles, sites of neighboring unit cells.

reported for a phase with the nominal composition $Li_{3.3}Mo_6S_8$ prepared by the butyllithium technique which concludes that the Li atoms essentially occupy the outer sites.[18] If we accept a similar structure model for the line phase $Li_3Mo_6S_8$, we arrive at a highly symmetric model in which every unit cell origin is surrounded by a trigonal cluster of Li in one plane of the puckered six ring of outer positions.

When the temperature dependence of the $^7Li$ NMR line shapes is measured, the second moment $M_2$ of the fixed lattice can be determined via the van Vleck relation, which allows an estimation of the Li–Li distances. If we start from two equidistant neighboring nuclei, the distances between the Li atoms within one $Li_3$ cluster can be estimated to ca. 270 pm.[15] Positions on neighboring outer sites between two different hexagons cannot be occupied simultaneously due to the small distance between these sites, so that an overall trigonal pattern of high symmetry results (Figure 5).

In order to demonstrate the unusual magnitude of the chemical shift of $Li_3Mo_6S_8$, we have collected data from the literature[20,21] and have measured the shift values for a large series of ternary phases $Li_xM_yX_z$ (M = transition metal, X = nonmetal);[15] selected data for chalcogenides are given in Figure 4b. General trends observed are (i) an increase in $\delta$ (diamagnetic shielding) with increasing electronegativity of the lattice anion X, ternary lithium oxides exhibiting values in the range of +6 to +37 ppm vs. LiCl, while the corresponding sulfides and selenides are found in the range of 0 to −30 ppm, and (ii) a decrease in $\delta$ with increasing lithium content for a given phase with variable Li stoichiometry. The lowest value reported so far for a lithium/non-metal compound is −42 ppm in the case of the graphite intercalation compound $LiC_6$.[22] It is obvious from this comparison that the negative shift values observed for $Li_3Mo_6S_8$ (and similarly for $Li_3Mo_6Se_8$; cf. below) are unusually large. With decreasing temperature an additional significant increase in negative shift has been observed ($\delta$ = −100 at 135 K).[15]

We interpret the extreme shift of $Li_3Mo_6S_8$ as a Knight shift, i.e. in terms of residual s electron density at the lithium nuclei and a formal oxidation state below +1. The formation of guest clusters via metal–metal bonding in intercalation systems has been discussed earlier.[4,23] It may appear in cases where the number of electrons transferred exceeds the maximum number of electrons that can be accepted by the host band; however, if the total energy of the system is lowered, it may occur also in cases where the band is not filled up completely. In the extreme case of $Tl_xV_5S_8$, there is no net charge transfer to or from the host band and the redox reaction proceeds exclusively via a change in the oxidation state of the guest cation between +1 and +3.[24] Lithium cannot have an integral positive oxidation state below +1; we explain the strong Knight shift therefore with the formation of clusters $(Li_3)^{2+}$, i.e. one-electron/three-center bonding with an average formal oxidation state for Li of $+^2/_3$. As mentioned already, the distance between Li atoms within one $Li_3$ cluster is estimated to ca. 270 pm.

The Li–Li distance observed in lithium metal is equivalent to 310 pm; the corresponding values for isolated $Li_3^0$ clusters (296 pm) and $Li_3^+$ clusters (308 pm) with triangular geometry have been calculated by Gole et al.[19] The value discussed above for the $(Li_3)^{2+}$ cluster in $Li_3Mo_6S_8$ is therefore geometrically compatible with a Li–Li bonding interaction. The bonding model proposed would thus be consistent with (i) the large Knight shift, (ii) the most likely geometrical arrangement of Li, and (iii) the estimated bond length between Li atoms within $Li_3$ clusters. On the basis of ionic formulas, the representation of $Li_3Mo_6S_8$ with *partial* charge transfer corresponds to structure a, while structure b describes the case of *quantitative* charge transfer:

$$\underset{a}{(Li_3)^{2+}[Mo_6S_8]^{2-}} \qquad \underset{b}{(Li^+)_3[Mo_6S_8]^{3-}}$$

On addition of a fourth lithium to the system the only available positions are those on the inner hexagonal ring of vacant sites. Due to the contraction of the *c* axis the sulfur atoms of neighboring $Mo_6S_8$ clusters lying on the threefold symmetry axis (i.e. close to the unit cell origin) come closer to each other and thus strongly affect Li atoms residing on inner positions. This effect must correlate in some way with the significant decrease in negative shift from $Li_3$ to $Li_{3.8}$: the symmetry of the Li arrangement is perturbed, and changes in hybridization may result. Although due to the minor changes in the lattice parameters appearing in this range, potential one- or two-phase systems cannot be clearly identified by X-ray measurements, Li NMR data prove the existence of intermediate states (Figure 2d).

The very high shift value measured for the terminal phase $Li_4Mo_6S_8$ suggests the presence of "simple" $Li^+$ ions, i.e. quantitative charge transfer according to

$$(Li^+)_4[Mo_6S_8]^{4-}$$

The sudden strong change in shift at $x = 4$ is probably related to the metal/semiconductor transition induced on saturation of the electron-deficient $Mo_6$ cluster with 24 electrons.

**IV. The Selenide System Li/$Mo_6Se_8$.** The behavior of $Mo_6Se_8$ with respect to intercalation of lithium is closely similar to that of the sulfide, which is rather surprising in terms of the charge-transfer model proposed by Yvon that predicts a decrease in the upper intercalation limit of ternary atoms with increasing atomic number of the chalcogen anion.[1] In Figure 6a the potential/charge-transfer diagram is given which illustrates that the endpoint of the reaction corresponds to $Li_4Mo_6Se_8$, i.e. a formal charge transfer of $4e/Mo_6Se_8$. The integral analytical lithium content $\bar{x}$ is almost linearly correlated with the charge transfer over the whole range (Figure 6b), and side reactions can thus be excluded. The maximum uptake of four Li per $Mo_6Se_8$ is in agreement with our former studies[25] and with a recent electrochemical investigation by McKinnon et al.,[26] while Tarascon et al. reported an upper limit of $Li_{3.2}Mo_6Se_8$.[9] Sections I and II (Figure 6a) are two-phase regions with the coexisting phases $Mo_6Se_8/Li_1Mo_6Se_8$ and $Li_1Mo_6Se_8/Li_3Mo_6Se_8$, respectively. This is supported by the structural data given in Figure 6c and Table I. McKinnon et al.[27]

(18) Cava, R. J.; Santoro, A.; Tarascon, J. M. *J. Solid State Chem.* **1984**, *54*, 193.
(19) Gole, J. L.; Childs, R. H.; Dixon, D. A.; Eades, R. A. *J. Chem. Phys.* **1980**, *72*, 6368.
(20) Silbernagel, B. G. *Solid State Comm.* **1975**, *17*, 361.
(21) Silbernagel, B. G.; Whittingham, M. S. *Mater. Res. Bull.* **1977**, *12*, 853.
(22) Conard, J.; Estrade, H. *Mater. Sci. Eng.* **1977**, *31*, 173.
(23) Schöllhorn, R. *Comments Inorg. Chem.* **1983**, *2*, 271.
(24) Schramm, W.; Schöllhorn, R.; Eckert, H.; Müller-Warmuth, W. *Mater. Res. Bull.* **1983**, *18*, 1283.
(25) Dolscheid, P. Dissertation Universität Münster 1983.
(26) Dahn, J. R.; McKinnon, W. R.; Coleman, S. T. *Phys. Rev. B: Condens. Matter* **1985**, *31*, 484.
(27) Dahn, J. R.; McKinnon, W. R. *Phys. Rev. B:* Condens. *Matter* **1985**, *32*, 3003.

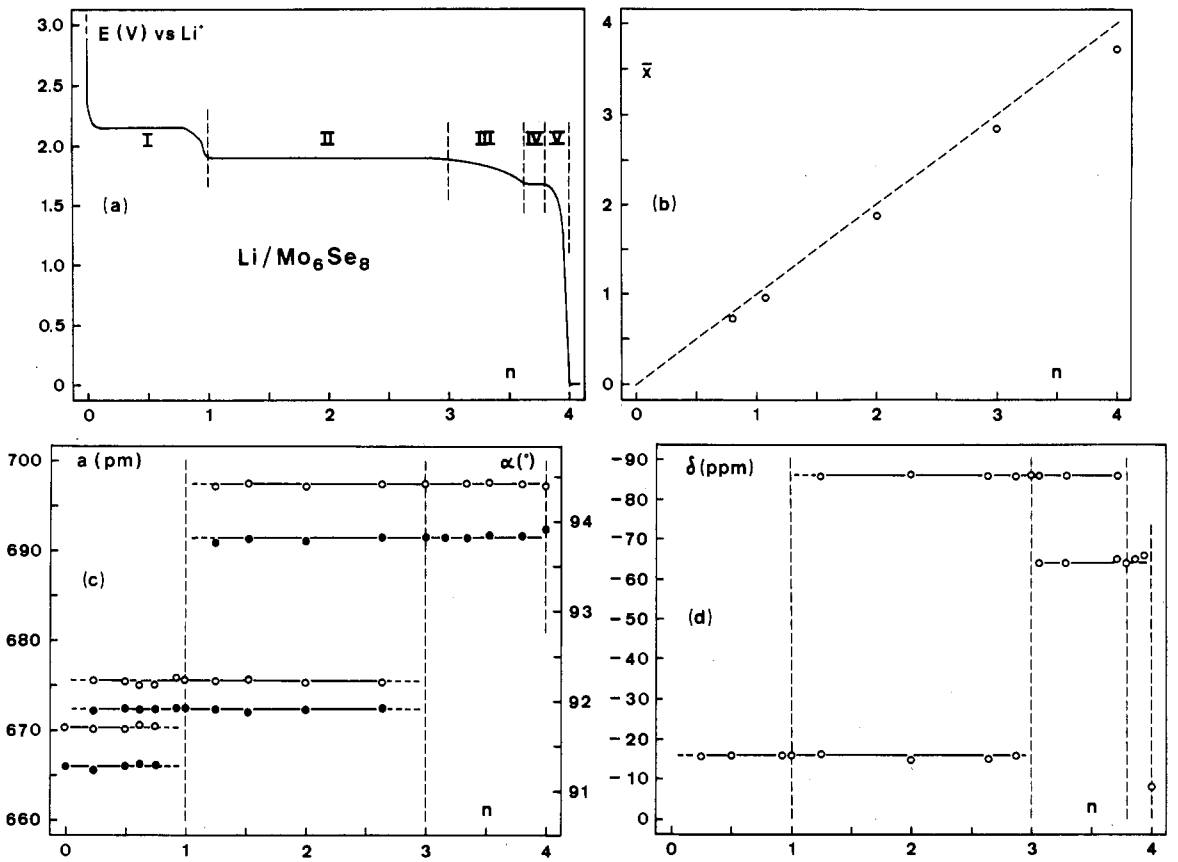


**Figure 6.** Formation of $Li_xMo_6Se_8$ by galvanostatic cathodic reduction of $Mo_6Se_8$ electrodes (conditions as indicated in Figure 2): (a) change of potential $E$ with the charge transfer $n$ (e/$Mo_6Se_8$); (b) correlation between the integral Li content $\bar{x}$ of the reaction products with $n$; (c) change of rhombohedral lattice parameters with $n$ ($a_R$ = ●, $\alpha_R$ = ○); (d) $^7$Li NMR phase diagram (300 K), change of the chemical shift with $n$.

observed a one-phase region $Li_xMo_6Se_8$ with $0 \leq x \leq 1$, which was analyzed in terms of a lattice gas model. These data cannot be confirmed by the present study. The reactions appearing in sections I and II can be described by eq 6 and 7.

$$Li^+ + e^- + Mo_6Se_8 \rightleftarrows Li_1[Mo_6Se_8] \quad (6)$$

$$2Li^+ + 2e^- + Li_1Mo_6Se_8 \rightleftarrows Li_3[Mo_6Se_8] \quad (7)$$

For sections III–V the electrochemical data suggest one two-phase region (IV) and two one-phase regions (III and V) (Figure 6a). The lattice parameters, which remain essentially constant up to $n = 4$, do not allow a discrimination. The NMR phase diagram confirms the existence of two-phase regions in sections I and II (Figure 6d). However, a clear two-phase region is also found in the range $3 \leq n \leq 3.8$, while only one signal ($\delta = -64$) appears in the range $3.8 \leq n \leq 3.98$. For $n = 4$ the shift value decreases significantly to $\delta = -8$.

The phase $Li_3Mo_6Se_8$ is thus in terms of NMR data again clearly a line phase. Strong changes are found for $\alpha_R$, $c/a$, and $V$ relative to those for the binary phase $Mo_6Se_8$ (Table I). The change in unit cell volume (11.3%) is by far the highest observed for all ternary phases $A_xMo_6Se_8$ reported. While the chemical shift of $Li_1Mo_6Se_8$ ($\delta = -16$) is consistent with the presence of $Li^+$ ions, the unusual magnitude of the shift of $^7$Li in $Li_3Mo_6Se_8$ with $\delta = -86$ indicates significant s electron density at the lithium nuclei, which can be interpreted—as in the case of the sulfide compound—by a high symmetry of the lithium arrangement and the formation of $(Li_3)^{2+}$ clusters with electron-deficient multicenter metal bonding. A recent powder neutron diffraction study on the compound $Li_{3.2}Mo_6Se_8$ (prepared via butyllithium)[18] concludes that the Li atoms are located essentially on sites of the outer six ring around the unit cell origin.

The addition of one extra lithium to the $Li_3$ system breaks the symmetry and results in changes of the bonding character, which effect reduced s electron density at the lithium sites and thus considerably lower values of the Knight shift (sections III–V).

The reactions of $Mo_6Se_8$ are reversible, and on anodic oxidation the same sequence of phases as found on reduction reappears without hysteresis in the inverse sense; this is true also for the NMR data. The product of quantitative oxidation is again $Mo_6Se_8$ with the original lattice parameters. As expected, the free energies $\Delta G$ of the selenide system are smaller as compared to those of the sulfides (Table II).

**V. Ionic Mobility.** The NMR studies confirm our earlier conclusions of a rather high mobility of lithium in these host lattices at ambient temperature based on cyclic voltammetric investigations.[7] The line widths (half-width at half-intensity) lie between 400 and 800 Hz for $Li_xMo_6S_8$ and between 500–1200 Hz for $Li_xMo_6Se_8$; the larger values belong to $x = 3.8$ and $x = 4$. Line broadening upon cooling does not occur down to temperatures of 80 K. The spin–lattice relaxation rates have their maxima at temperatures between 140 and 200 K. From both line width and relaxation data activation energies on the order of magnitude of 10 kJ mol$^{-1}$ are derived. There is no important dependence upon the stoichiometry.[15]

Measurements of the chemical diffusion coefficient $\tilde{D}$ by the galvanostatic intermittent titration technique[28] yielded values of $10^{-7}$ to $10^{-9}$ cm$^2$ s$^{-1}$ for $Li_1Mo_6S_8$ and $Li_3Mo_6S_8$, i.e. a slight decrease of $\tilde{D}$ with increasing Li content, while in the case of the selenide ($\tilde{D} = 10^{-8}$ cm$^2$ s$^{-1}$) no change with the variation in stoichiometry from $x = 1$ to $x = 3$ was observed. Measurements on the $Li_{3.8}$ and $Li_{4.0}$ phases did not yield conclusive results because of the nonideal behavior of the relaxation curves. The values measured are comparable with those found for lithium ions in layered transition-metal dichalcogenides at ambient temperature, e.g. $Li_xTiS_2$ with $\tilde{D} = 5 \times 10^{-9}$ cm$^2$ s$^{-1}$ over the entire composition range and $Li_xTaS_2$ with $\tilde{D} = 1.8 \times 10^{-8}$ cm$^2$ s$^{-1}$ as the average value in the composition range $0.25 < x < 0.75$.[29] It is surprising

(28) Weppner, W.; Huggins, R. A. *Annu. Rev. Mater. Sci.* **1978**, *8*, 269.

that the strong change in lattice distortion, unit cell volume and occupation density of vacant sites from $Li_1$ to $Li_3$ phases is not reflected in the transport behavior.

**Conclusion.** The simple approach used for the description of solid-state reactions proceeding via electron/ion-transfer processes is based on the model of quantitative charge transfer; i.e., all electrons transferred to the solid via chemical or electrochemical action are accepted by the host lattice band.[4] This scheme involves obviously also the constraint of a rigid band model.

In the case of $Li/Mo_6S_8$ the maximum uptake of four $Li^+$ ions predicted by the ionic structure model as well as by the band structure is in fact observed. Extended investigations by us on the intercalation of other closed-shell ions (e.g. $Zn^{2+}$, $Cd^{2+}$) and transition-metal ions gave evidence that under appropriate conditions the maximum electrochemical charge transfer is equivalent to $4e/Mo_6S_8$ in those cases.[3,4,7] As mentioned already above, the situation may be more complex, however. In the case of $Ni_2$-$H_2Mo_6S_8$ the electrochemical charge transfer measured amounts to $6e/Mo_6S_8$. The rigid band model can be maintained, however, if partial "storage" in guest/guest bonding (Ni/H) of the electrons transferred is assumed, i.e. only a fraction of the total number of electrons accepted by the solid is taken up by the host band.[4,23,30,31] Similar cases of partial charge transfer have been reported for other host lattices, e.g. $Tl_xV_5S_8$.[24] A related situation is found in the system under discussion, where the extreme chemical shift value of the $Li_3Mo_6X_8$ phases has been discussed in terms of partial charge transfer ("Knight shift"), i.e. $(Li_3)^{2+}[Mo_6X_8]^{2-}$. There is still a further point that merits attention. The ionic model proposed by Yvon[1] concludes that the maximum electron transfer to the $Mo_6X_8$ matrix should decrease with decreasing electron affinity of the chalcogen ions in the series $S \rightarrow Se \rightarrow Te$. The results of the present study show, however, a formal maximum transfer of 4e (assuming quantitative transfer) also in the case of the selenide. In fact the Pauling electronegativities of S and Se are not strongly different, while the value for Te is much lower. We found actually that upon intercalation of Li in $Mo_6Te_8$ the stoichiometry obtained for $Li_xMo_6Te_8$ is below $x = 2$. This may be due, however, to lattice disorder in the binary phase prepared at high temperatures, which leads to blocked lattice channels. We are presently performing a study on lithium intercalation in $Mo_6Te_8$ prepared from the first ternary phase $Ni_{0.8}Mo_6Te_8$ reported recently[32] in order to clear up this point.

It is obvious that we are presently not yet able to understand the behavior of these complex systems on a satisfactory level. Refined structural studies and the application of a variety of physical methods able to yield information on the charge transfer are required. The investigation of $Mo_6$ type cluster chalcogenides with their unusual properties in terms of the correlation of structure/bonding/chemical reactivity remains certainly an interesting field in many respects, e.g. the use of these phases as highly variable model systems for the understanding of solid-state reactions of electronic conductors at room temperature, the synthesis of new metastable phases not accessible by conventional preparation, the modification of physical properties of a given solid by reversible chemical reactions at ambient temperature, and the variation of the catalytic activity of $Mo_6$ cluster phases.[4]

(29) Basu, S.; Worrell, W. L. In *Fast Ion Transport in Solids*; Vashishta, P., Mundy, J. N., Shenoy, G. K., Eds.; North Holland: New York, 1979, p 149.
(30) Schöllhorn, R. In *Physics of Intercalation Compounds*; Pietronero, L., Tosatti, E., Eds.; Springer Verlag: Berlin, New York, 1981; p 33.
(31) Schramm, W.; Gocke, E.; Schöllhorn, R. *Mater. Res. Bull.* **1986**, *21*, 929.
(32) Hönle, W.; Yvon, K. *Z. Kristallogr.* **1983**, *162*, 103.